Orbit-Coupled Multiphysics Degradation Modelling of CubeSat Lithium-Ion Batteries

Aswin KARKADAKATTIL*

*Corresponding author
Independent Researcher, Kasaragod, Kerala 671314, India,
ashwinharik20000@gmail.com

DOI: 10.13111/2066-8201.2026.18.1.4

Received: 01 February 2026/ Accepted: 23 February 2026/ Published: March 2026

Abstract: *CubeSats operate under severe orbital thermal cycling and limited thermal control authority, making lithium-ion battery degradation a primary mission-limiting factor. Repeated sunlight–eclipse transitions in low Earth orbit induce high-frequency temperature oscillations, while progressive internal resistance growth amplifies Joule heating over multi-year operation. Existing degradation models typically treat electrochemical aging and thermal behaviour independently, neglecting cumulative orbit-coupled feedback mechanisms that drive nonlinear lifetime reduction. This study presents a Multiphysics, orbit-resolved cumulative degradation framework that integrates Arrhenius temperature dependence, current-induced electrochemical stress, resistance growth, and transient thermal balance within a unified differential formulation. The model captures progressive coupling between heat generation, temperature rise, and degradation kinetics across mission-scale timescales. Results demonstrate pronounced nonlinear capacity fade, convex resistance acceleration near end-of-life, and thermal amplification effects that substantially reduce predicted mission duration. Sensitivity analysis identifies activation energy and orbital current amplitude as dominant reliability drivers. The proposed framework enables physics-consistent mission lifetime prediction and provides a quantitative design tool for CubeSat power system optimization, reliability assessment, and thermal margin evaluation under realistic orbital forcing conditions.*

Key Words: *CubeSat power systems, lithium-ion battery degradation, orbit-coupled thermal modelling, Arrhenius aging kinetics, Multiphysics reliability analysis, nonlinear capacity fade, resistance growth amplification, mission lifetime prediction*

1. INTRODUCTION

1.1 CubeSat Power Reliability Challenges

CubeSats have emerged as cost-effective and rapidly deployable platforms for scientific, commercial, and technology demonstration missions [20]. Their compact architecture enables rapid development cycles; however, this miniaturization imposes severe constraints on thermal control capability, structural mass, and onboard energy storage capacity. Lithium-ion batteries are widely adopted in CubeSat power systems due to their high specific energy and maturity. Nevertheless, their performance is highly sensitive to temperature and cycling stress. In low Earth orbit (LEO), a typical CubeSat undergoes approximately 14–16 sunlight–eclipse transitions per day. These periodic transitions induce repeated temperature oscillations within the spacecraft structure and battery pack [6, 14]. Unlike larger spacecraft equipped with active thermal control subsystems, CubeSats predominantly rely on passive heat dissipation strategies, including conduction paths, surface coatings, and radiative elements [7, 16, 17]. Active thermal control architectures have also been investigated for CubeSat platforms, although their implementation remains constrained by mass and power limitations [10]. The limited structural mass and reduced heat rejection area amplify temperature fluctuations, thereby increasing thermally activated degradation rates. Thermal management strategies for CubeSats have been widely studied, particularly through the use of phase change materials (PCMs) and passive thermal architectures [1–4, 11, 12, 23]. AI-assisted hybrid thermal regulation approaches have also been proposed to enhance CubeSat temperature stabilization under orbital forcing conditions [44]. While these approaches address peak temperature mitigation, they do not explicitly quantify long-term electrochemical degradation or mission-scale lifetime reduction. Meanwhile, studies on battery thermal management in terrestrial systems emphasize the importance of temperature control in mitigating capacity fade and internal resistance growth [26]. For CubeSat platforms, the combined effect of orbit-scale thermal cycling, progressive internal resistance increase, and Joule heating amplification can significantly accelerate electrochemical aging. The reduced battery mass inherent to nanosatellite architectures further increases effective C-rate stress relative to larger spacecraft systems. Consequently, battery degradation frequently becomes a primary mission-limiting factor, directly influencing payload duty cycles and communication reliability [19], as well as end-of-life (EOL) thresholds. Accurate prediction of degradation under realistic orbital forcing is therefore essential for mission assurance, power budgeting accuracy, and reliability-driven spacecraft design.

1.2 State of the Art

Battery degradation modelling has been extensively developed in terrestrial domains, particularly for electric vehicles and grid storage systems. These models commonly employ Arrhenius-type temperature dependence combined with empirical cycle-life relationships to estimate capacity fade and internal resistance growth [26]. Such approaches effectively capture thermally activated aging mechanisms under controlled ambient conditions. In parallel, spacecraft thermal modelling has evolved to predict temperature distributions under orbital radiation loads, eclipse transitions, and passive heat rejection constraints [6, 14, 17]. Environmental load estimation techniques have also been implemented using numerical tools such as MATLAB to evaluate CubeSat temperature profiles [5]. Within CubeSat research, thermal management solutions including PCM integration, additive manufacturing enhancements, and passive radiator systems have been widely explored [1–4, 11, 16]. Paraffin-based materials have also been studied extensively in aerospace thermal and propulsion contexts, demonstrating strong thermo-physical sensitivity under cyclic loading [22, 24]. Advanced material systems such as phase-change photonic materials have further expanded the design space for thermally adaptive spaceborne systems [21]. Broader aerospace thermal studies, including high-speed aircraft and satellite cooling analyses, have examined heat rejection efficiency and advanced cooling concepts relevant to orbital environments [27, 30]. Micro-scale thermal transport and capillary-driven flow mechanisms have similarly been investigated for enhanced aerospace heat management [29]. However, these modelling domains have largely progressed independently. In many aerospace applications, battery aging is approximated as an algebraic function of mission time or cycle count, without explicit coupling to transient temperature evolution. Conversely, terrestrial battery models typically assume controlled environmental conditions and do not incorporate orbit-driven thermal forcing or spacecraft-specific load variations. Recent advances in physics-informed modelling

and real-time spacecraft thermal simulation demonstrate growing interest in integrated system-level approaches [9]. Nevertheless, no existing framework simultaneously integrates:
• Orbit-resolved transient thermal forcing,
• Differential cumulative degradation kinetics,
• Resistance-driven Joule heating feedback, and
• Mission-level reliability threshold evaluation.
To clarify the positioning of the present work, Table 1 summarizes representative modelling categories in existing literature and highlights the absence of a fully integrated orbit-coupled Multiphysics degradation framework.

Table 1. Comparative assessment of CubeSat battery degradation modelling approaches

Modelling Category	**Transient Thermal Modelling**	**Electrical–Thermal Coupling**	**Differential Cumulative Aging**	**Orbit-Resolved Forcing**	**Mission-Level Reliability**
Empirical time-based aging models	No	No	No	No	Limited
Lumped steady-state thermal models [6, 14]	Partial	No	No	No	No
PCM-based thermal management studies [1–4, 11]	Yes	No	No	No	No
Electrochemical degradation models (terrestrial) [26, 31–43]	Temperature -dependent	Partial	Yes	No	Limited
Present Work	Yes	Yes	Yes	Yes	Yes

The comparative assessment demonstrates that existing approaches either neglect orbit-scale thermal forcing, omit cumulative differential degradation kinetics, or exclude resistance–temperature feedback effects. No prior framework integrates these components into a unified mission-level reliability model tailored to CubeSat operating conditions.

1.3 Research Gap

Although lithium-ion degradation kinetics and spacecraft thermal behaviour have been individually investigated, the coupled influence of orbit-scale thermal cycling and cumulative electrochemical aging remains insufficiently modelled in CubeSat applications. Existing approaches typically represent degradation as an algebraic function of mission time or cycle count, independent of evolving resistance and temperature feedback. Such simplifications neglect nonlinear amplification mechanisms arising from resistance-induced Joule heating and Arrhenius-driven temperature sensitivity. As degradation progresses, internal resistance increases, enhancing heat generation, elevating operating temperature, and further accelerating aging - a feedback loop that is not resolved in conventional time-based models. A physics-consistent, cumulatively integrated Multiphysics framework is therefore required to accurately predict CubeSat battery lifetime under realistic orbital conditions and to quantify mission reliability margins.

1.4 Contributions and Novelty

This study addresses the identified gap through the following contributions:

- Development of a cumulative differential degradation model incorporating Arrhenius temperature dependence and current-induced stress within a mission-scale integration framework.
- Integration of orbit-resolved transient thermal forcing to capture sunlight–eclipse cycling effects on battery temperature evolution.

- Implementation of coupled resistance–capacity feedback linking degradation progression with Joule heating amplification and thermal drift.
- Quantitative mission-scale reliability evaluation enabling prediction of end-of-life thresholds under realistic CubeSat operating profiles.

Novelty Clarification

The novelty of this work does not lie in introducing new electrochemical reaction mechanisms, but in integrating established degradation kinetics with orbit-resolved thermal forcing and resistance feedback into a unified, cumulatively integrated reliability framework. Unlike algebraic time-based aging models, the proposed approach:

1. Resolves short-term orbital temperature oscillations.
2. Integrates degradation through a differential formulation.
3. Captures nonlinear amplification arising from thermo-electrical coupling.
4. Directly links physics-based degradation evolution to mission-level reliability thresholds.

This integrated perspective enables physics-consistent mission lifetime prediction under realistic CubeSat operational constraints.

2. BACKGROUND AND THEORETICAL FRAMEWORK

2.1 Orbital Thermal Environment of CubeSats

CubeSats operating in Low Earth Orbit (LEO) experience a highly dynamic thermal environment driven by repeated sunlight–eclipse transitions. A typical 90-minute orbit results in approximately 14–16 thermal cycles per day. During sunlit phases, absorbed solar radiation and reflected Earth albedo elevate spacecraft temperature, while eclipse periods lead to rapid radiative cooling toward deep-space background conditions. Unlike larger spacecraft platforms, CubeSats generally lack active thermal control subsystems due to strict mass and volume constraints. Instead, they rely primarily on passive mechanisms such as:

- Conduction through structural members
- Surface emissivity optimization
- Passive radiative heat rejection

Because of their limited structural mass and low thermal inertia, CubeSats are more susceptible to transient temperature fluctuations. These variations are often amplified at the component level, particularly within battery packs. As a result, battery temperature evolves continuously with orbital phase rather than remaining near steady-state conditions. Such cyclic thermal oscillations directly influence electrochemical reaction kinetics and accelerate thermally activated degradation processes. Consequently, time-resolved thermal modelling is essential for accurately capturing realistic operating conditions, as steady-state approximations fail to represent orbit-driven thermal behaviour.

2.2 Lithium-Ion Battery Degradation Mechanisms

Lithium-ion battery aging results from multiple interacting physicochemical processes. While detailed electrochemical modelling may involve multi-scale porous electrode theory, mission-level prediction typically relies on lumped degradation kinetics that capture dominant mechanisms. The most widely recognized degradation pathways include:

- Solid Electrolyte Interphase (SEI) growth
- Loss of active lithium inventory
- Structural electrode degradation
- Lithium plating under elevated current stress

Among these, SEI growth is widely regarded as a principal contributor to long-term capacity fade and internal resistance increase in graphite-based lithium-ion systems. Both theoretical and experimental investigations have shown that SEI formation progresses through diffusion- and reaction-controlled processes and is closely associated with impedance rise and performance decay [31–33, 38, 40, 43]. The temperature dependence of degradation rate is commonly described using Arrhenius-type kinetics:

$$k(T) \propto \exp\left(-\frac{E_a}{R_g T}\right) \tag{1}$$

where E_a denotes the apparent activation energy associated with parasitic side reactions such as electrolyte decomposition and SEI thickening.

Experimental Arrhenius analyses consistently report activation energies in the range of 35–50 kJ/mol under moderate temperature exposure [37, 41, 42]. Differential formulations of SEI-driven degradation have also been proposed to capture temperature-dependent aging behavior more realistically [39, 43]. In terrestrial applications such as electric vehicles and stationary storage systems, environmental conditions are typically regulated. In contrast, CubeSat batteries operate under fundamentally different constraints. Rapid temperature transitions, relatively high effective C-rates due to limited battery mass, and restricted heat dissipation pathways combine to create coupled electro-thermal stress conditions. Experimental studies conducted under varying C-rates confirm accelerated degradation and impedance growth at higher current densities [35–37], supporting the inclusion of current-dependent stress terms in mission-level degradation models.

2.3 Arrhenius-Based Cumulative Aging Formulation

Mission-level degradation modelling is often expressed through empirical relationships of the form:

$$D(t) = f(t, T, I) \tag{2}$$

where degradation depends on time, temperature, and current.

In many aerospace applications, aging is approximated algebraically as proportional to mission time or cycle count. Although computationally efficient, such formulations neglect evolving interactions between resistance growth, heat generation, and temperature changes.

A more physically consistent representation treats degradation as a cumulative process governed by a differential formulation:

$$\frac{dD}{dt} = g(T, I) \tag{3}$$

Similar differential SEI-based aging formulations have been investigated in electrochemical modelling studies [31–33, 39, 43], demonstrating improved capability in capturing nonlinear aging behavior compared to purely algebraic approaches. By integrating degradation incrementally over mission duration, this framework allows short-term orbital temperature oscillations to influence long-term lifetime evolution. In doing so, it captures nonlinear amplification mechanisms that naturally arise in coupled electro-thermal systems.

2.4 Electro–Thermal Feedback Mechanisms

As degradation progresses, internal resistance increases. Experimental impedance measurements consistently demonstrate progressive resistance growth correlated with SEI thickening and structural aging [38, 42].

This resistance growth has direct thermal implications:

- Joule heat generation increases
- Operating temperature rises
- Arrhenius-driven degradation accelerates

These effects create a positive feedback loop:

$$R_{int} \uparrow \Rightarrow Q_{gen} \uparrow \Rightarrow T \uparrow \Rightarrow D \uparrow \quad (4)$$

Such coupled amplification behavior has been observed experimentally under accelerated aging and high-rate charging conditions [35, 36]. However, this interaction is rarely resolved within orbit-scale thermal forcing conditions specific to CubeSat missions.

Accurate modelling therefore requires simultaneous treatment of:

- Thermal energy balance
- Degradation kinetics
- Resistance evolution
- Capacity fade relationships

Without this integrated approach, mission lifetime predictions may underestimate degradation under realistic orbital operating conditions.

2.5 Mission-Level Reliability Metrics

In spacecraft applications, battery health must ultimately be interpreted in terms of mission reliability. End-of-life (EOL) thresholds are commonly defined based on:

- Capacity retention (typically 70–80% of nominal capacity)
- Acceptable internal resistance growth
- Thermal stability margins

Calendar-life prediction methodologies for lithium-ion systems have been extensively studied in terrestrial contexts [41, 42], but these approaches generally assume relatively stable operating environments.

For CubeSat missions, degradation evolves under cyclic thermal forcing and progressive electro-thermal feedback. Reliability modelling must therefore connect cumulative degradation trajectories directly to mission duration and orbital operating conditions. Such linkage enables quantitative lifetime estimation, improved power budgeting accuracy, and more reliable mission planning under realistic CubeSat operating constraints.

3. METHODOLOGY

This section presents the coupled Multiphysics framework developed to model lithium-ion battery degradation in CubeSat missions. The formulation integrates orbit-resolved transient thermal forcing, electrically induced heat generation, cumulative degradation kinetics, and feedback-driven resistance evolution into a unified time-dependent system. The objective is to capture both short-term orbital temperature oscillations and long-term nonlinear aging amplification within a physics-consistent framework.

3.1 Orbital Thermal Model

The thermal behavior of the CubeSat battery pack is modelled using a lumped-capacitance energy balance formulation. This assumption is appropriate for nanosatellite architectures due to their limited structural mass and relatively small internal temperature gradients compared to orbital and mission-scale timescales. The approach enables system-level thermal prediction without resolving cell-level spatial gradients, which are secondary for long-duration degradation analysis. The governing thermal balance equation is expressed as:

$$C_{th}\frac{dT}{dt} = I^2R - hA(T - T_{env}) \tag{5}$$

where:
C_{th} is the effective thermal capacitance of the battery system ($J \cdot K^{-1}$),
T is the instantaneous battery temperature (K),
I is the battery current (A),
R is the internal resistance (Ω),
hA is the effective passive heat rejection coefficient ($W \cdot K^{-1}$),
T_{env} is the orbit-dependent environmental temperature (K).
The left-hand term represents transient thermal energy storage within the battery system. The right-hand side accounts for internally generated Joule heat and passive heat exchange with the surrounding spacecraft structure and radiative environment.

Sunlight–Eclipse Forcing

To resolve orbit-scale thermal dynamics, the environmental temperature $T_{env}$is modeled as a periodic function representing alternating sunlight and eclipse phases. During sunlight exposure, radiative heating elevates the effective environmental temperature.
During eclipse, reduced radiative input promotes cooling toward deep-space equilibrium conditions. For Low Earth Orbit (LEO) conditions, a representative orbital period of approximately 90 minutes is assumed, with a sunlight fraction between 55–65%.
This periodic forcing induces cyclic thermal oscillations in the battery temperature consistent with typical CubeSat operating environments.
Unlike steady-state spacecraft thermal models, this transient formulation captures repeated orbital thermal loading that directly influences temperature-dependent degradation kinetics over multi-year missions.

Joule Heating and Nonlinear Feedback

The term I^2R represents resistive (Joule) heating generated during both charging and discharging cycles. Importantly, internal resistance R is not constant but evolves as a function of cumulative degradation.
As degradation progresses:

- Internal resistance increases,
- Joule heat generation rises for the same current amplitude,
- Operating temperature increases,
- Arrhenius-governed degradation accelerates.

This interaction introduces a nonlinear thermo-electrical feedback mechanism. The closed coupling between resistance growth and temperature elevation produces progressive thermal drift and nonlinear lifetime reduction that cannot be captured using decoupled or algebraic aging formulations.

Modelling Assumptions

The lumped thermal approximation assumes spatial temperature uniformity within the battery pack. While localized temperature gradients may arise under high current conditions, the present framework focuses on mission-scale degradation behavior rather than microthermal effects within individual cells. This level of abstraction is appropriate for system-level reliability prediction and aligns with common CubeSat thermal modelling practices. Orbit-coupled thermo-electrochemical feedback framework for CubeSat battery degradation is shown in figure 1.

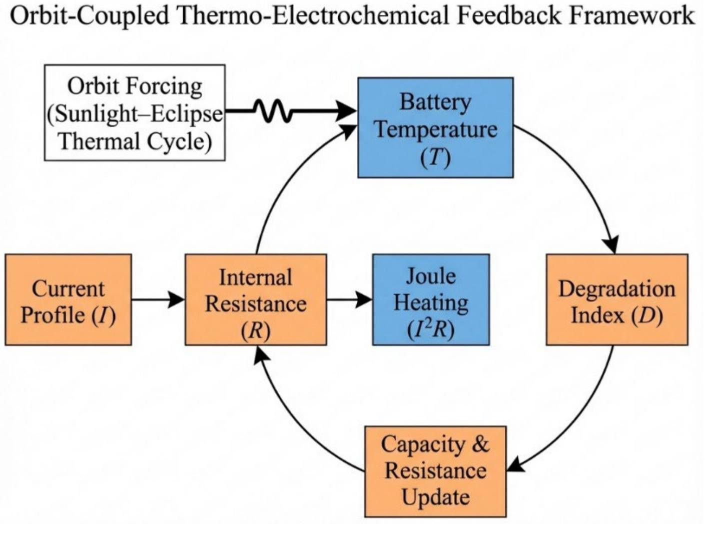

Figure 1. Orbit-coupled thermo-electrochemical feedback framework for CubeSat battery degradation.

Schematic representation of the coupled Multiphysics interactions governing mission-scale aging. Orbital current loading drives internal resistance, which produces Joule heating. Elevated temperature accelerates electrochemical degradation through Arrhenius kinetics, increasing the degradation index and further amplifying internal resistance. The closed feedback loop captures nonlinear lifetime acceleration not represented in uncoupled or algebraic degradation models.

3.2 Cumulative Degradation Model

Electrochemical degradation is modelled using a cumulative differential formulation that captures thermally activated aging mechanisms and current-induced stress. The degradation rate is defined as:

$$\frac{dD}{dt} = k_0 \mid I \mid^m \exp\left(-\frac{E_a}{R_g T}\right) \tag{6}$$

where:
$D(t)$ is the cumulative degradation index,
k_0 is the pre-exponential degradation constant,
m is the current stress exponent,
E_a is the activation energy (J·mol^{-1}),
R_g is the universal gas constant,
T is the instantaneous battery temperature (K).

Arrhenius Temperature Dependence

The exponential Arrhenius term represents thermally activated electrochemical degradation processes such as solid-electrolyte interphase (SEI) growth, electrolyte decomposition, and impedance rise. Elevated temperature increases reaction kinetics exponentially, leading to nonlinear acceleration of degradation. The activation energy E_a was selected within the range of 40–45 kJ/mol, consistent with experimentally reported values for SEI growth in graphite-based lithium-ion chemistries under moderate temperature exposure. This range is widely observed for commercial graphite/NMC and graphite/LFP cells operating under combined calendar and cycling conditions. SEI formation is generally recognized as the dominant aging mechanism in lithium-ion batteries subjected to moderate thermal amplitudes. The CubeSat mission environment considered in this study corresponds to a Low Earth Orbit (LEO) platform with a 90-minute orbital period, producing repeated sunlight–eclipse transitions. Under passive thermal control, the battery temperature oscillates between approximately 255 K (eclipse cooling) and 308 K (sunlit heating). Within this moderate thermal range, SEI growth remains the primary degradation pathway, and activation energies in the range of 40–45 kJ/mol are therefore physically consistent with graphite-based lithium-ion chemistries typically employed in CubeSat battery systems.

Current Stress Contribution

The term $| I |^m$ captures the influence of cycling intensity. Higher current amplitudes increase electrochemical stress, promoting lithium plating, structural fatigue, and internal resistance growth. The exponent m reflects empirically observed sensitivity of degradation rate to C-rate in lithium-ion systems. Because CubeSat battery packs have relatively low mass and limited redundancy, effective C-rates can be higher than those encountered in larger spacecraft systems. Incorporating current-dependent stress therefore ensures that degradation accelerates appropriately under elevated load conditions.

Cumulative Integration

Unlike algebraic time-based aging models, the degradation index is obtained through explicit time integration:

$$D(t) = \int_0^t \frac{dD}{dt}\, dt \tag{7}$$

where:
This guarantees monotonic and physically consistent accumulation of damage. The differential formulation allows the degradation rate to vary dynamically with temperature and load, thereby capturing nonlinear aging transitions that arise from orbit-driven thermal oscillations and electro–thermal feedback.

3.3 Capacity and Resistance Evolution

Battery performance metrics are linked to cumulative degradation through linearized constitutive relationships:

$$\begin{aligned} C(t) &= C_0(1 - \beta D) \\ R(t) &= R_0(1 + \alpha D) \end{aligned} \tag{8}$$

where:

- C_0 and R_0 are initial capacity and resistance,
- β is the capacity degradation coefficient,
- α is the resistance growth coefficient.

Although linear in D, the overall system exhibits strongly nonlinear behavior due to the coupling between degradation, resistance growth, and temperature.
Nonlinear Amplification Mechanism
The nonlinear behavior arises from three interacting mechanisms:

1. Exponential Arrhenius dependence on temperature.
2. Resistance-driven amplification of Joule heating.
3. Orbit-scale periodic thermal forcing.

As degradation increases resistance, Joule heating rises. The elevated temperature accelerates degradation via the Arrhenius term, which further increases resistance. This closed feedback loop produces mission-scale nonlinear capacity fade and late-stage resistance acceleration. This mechanism differentiates the present model from uncoupled degradation formulations that assume constant resistance or steady temperature conditions.

3.4 Numerical Implementation

The coupled thermal and degradation equations are solved using explicit time integration with a fixed timestep corresponding to orbital resolution ($\Delta t \approx 60$ s). The simulation spans multi-year mission durations (typically three years), enabling resolution of both short-term orbital oscillations and long-term aging trends. At each timestep:

1. Orbital phase determines T_{env}.
2. The thermal equation updates temperature.
3. The degradation rate is computed using instantaneous temperature and current.
4. The degradation index is incremented.
5. Internal resistance and capacity are updated.
6. Joule heating is recalculated for the next timestep.

This sequential coupling ensures consistent interaction between thermal and electrochemical processes. Parameter values are selected based on representative lithium-ion battery properties reported in aerospace and electrochemical literature. Where direct mission data are unavailable, parameters are calibrated to reflect realistic multi-year CubeSat operation. Model Parameters and Baseline Values are shown in Table 2

Table 2 – Model Parameters and Baseline Values

Parameter	**Symbol**	**Value**	**Unit**	**Source/Justification**
Initial capacity	C_0	20	Wh	Representative CubeSat Li-ion pack
Initial resistance	R_0	0.05	Ω	Typical small-cell internal resistance
Activation energy	E_a	40–45 kJ/mol	$J \cdot mol^{-1}$	Lithium-ion aging kinetics literature
Pre-exponential factor	k_0	Calibrated	–	Mission-scale lifetime calibration
Current exponent	m	1.2–1.5	–	Empirical cycling sensitivity
Thermal capacitance	C_{th}	800–1000	$J \cdot K^{-1}$	Lumped battery pack estimate
Heat transfer coefficient	hA	0.1–0.2	$W \cdot K^{-1}$	Passive CubeSat thermal rejection
Capacity coefficient	β	0.3–0.5	–	Empirical capacity fade scaling
Resistance coefficient	α	1.5–2.0	–	Empirical resistance growth scaling

The selected parameter ranges ensure reproducibility and allow systematic sensitivity analysis across realistic CubeSat operating conditions.

4. RESULTS AND ANALYSIS

4.1 Mission-Scale Capacity Degradation

Figure 2 illustrates the evolution of battery capacity over a three-year mission duration under orbit-resolved transient thermal forcing. The capacity trajectory exhibits three distinct degradation regimes. During the initial phase (0–1.5 years), capacity decline appears approximately linear. In this regime, internal resistance remains relatively close to its initial value, and thermal oscillations remain bounded. Degradation progresses steadily but without significant amplification. Between approximately 1.5 and 2 years, a transition region emerges. Subtle curvature becomes visible in the degradation profile, indicating deviation from linear aging behavior. This inflection marks the onset of resistance-mediated thermal amplification. Beyond 2 years, a pronounced nonlinear acceleration in capacity fade is observed. The degradation curve steepens progressively as cumulative resistance growth increases Joule heating, elevating average operating temperature. Through the Arrhenius temperature dependence embedded in the degradation kinetics, even modest temperature increases result in exponential acceleration of aging processes. An 80% capacity retention threshold is included to define the operational end-of-life (EOL) criterion. The intersection of the degradation curve with this threshold provides a physics-based estimate of mission lifetime. Importantly, the onset of nonlinear curvature (“knee point”) occurs prior to threshold crossing, indicating that mission margin begins eroding well before formal EOL conditions are reached. These results demonstrate that degradation cannot be accurately represented using linear or algebraic time-based models under orbit-scale forcing. Neglecting the thermo-electrical feedback loop would significantly underestimate late-stage aging acceleration and overpredict mission lifetime.

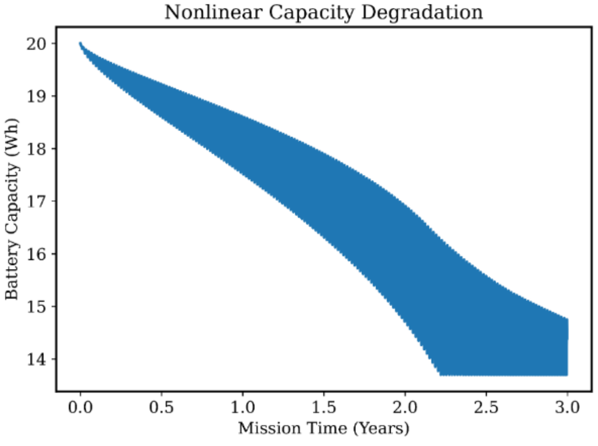

Figure 2. Mission-scale nonlinear capacity degradation under orbit-resolved thermal forcing

Evolution of battery capacity over a three-year CubeSat mission simulated using the coupled thermo-electrochemical degradation framework. Short-period oscillations correspond to sunlight–eclipse thermal cycling, while the long-term downward curvature reflects cumulative degradation. The pronounced acceleration beyond approximately two years indicates resistance-mediated thermal amplification, where increasing internal resistance enhances Joule heating, elevates operating temperature, and accelerates Arrhenius-driven aging kinetics. The late-stage steepening highlights the nonlinear nature of orbit-coupled degradation and the importance of integrated Multiphysics modelling for accurate mission lifetime prediction.
Battery capacity (Wh) versus mission time (years), including 80% end-of-life threshold and identified knee point indicating nonlinear acceleration.

4.2 Resistance Growth and Amplification

Figure 3 presents the temporal evolution of internal resistance over the three-year mission duration under orbit-resolved thermal forcing. The resistance trajectory exhibits pronounced convex upward curvature, indicating nonlinear amplification rather than linear aging. During the early mission phase, resistance growth is gradual and approximately linear with respect to time. In this regime, cumulative degradation remains moderate, and Joule heating contributions are relatively stable. As the mission progresses, the slope of the resistance curve increases steadily. Beyond approximately two years, a clear acceleration region emerges in which resistance rises sharply. This late-stage steepening reflects the cumulative integration of degradation kinetics coupled with temperature-dependent acceleration. The observed behavior confirms the feedback mechanism embedded in the Multiphysics framework. As degradation increases, internal resistance grows, which in turn amplifies resistive heat generation through the I^2R term. Elevated Joule heating increases battery temperature, and through the Arrhenius dependence of the degradation rate, accelerates further aging. This closed thermo-electrical loop produces the nonlinear resistance escalation observed near end-of-life. From an engineering perspective, accelerated resistance growth directly affects voltage stability, peak power capability, discharge efficiency, and thermal safety margins. The results indicate that resistance evolution not only capacity fade must be considered in mission-level reliability assessment for CubeSat power systems.

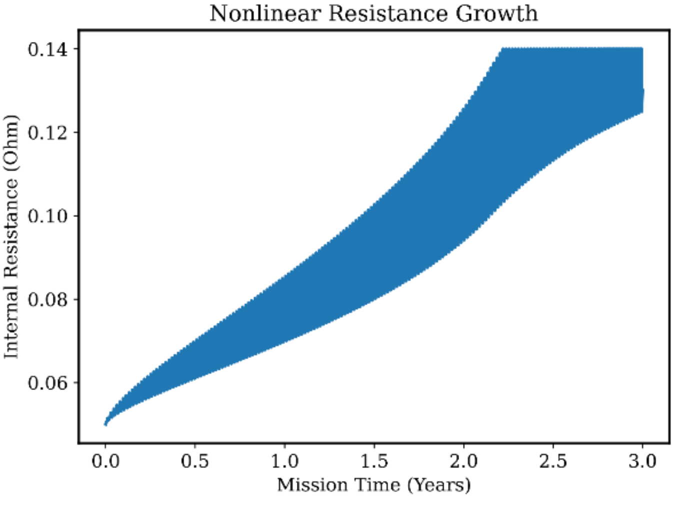

Figure 3. Nonlinear internal resistance growth under orbit-coupled degradation

Temporal evolution of battery internal resistance over the mission duration. The convex upward profile demonstrates late-stage acceleration driven by cumulative degradation and Joule-heating-induced thermal amplification. The sharp rise near end-of-life highlights the nonlinear feedback between resistance growth and temperature-dependent aging kinetics.

4.3 Orbit-Resolved Thermal Evolution

Figure 4 illustrates the battery temperature response over the full three-year mission duration under periodic sunlight–eclipse forcing. High-frequency oscillations correspond directly to orbital transitions, reflecting alternating radiative heating during sunlight exposure and cooling during eclipse phases. These periodic fluctuations are consistent with the assumed 90-minute low Earth orbit cycle and confirm that the model resolves orbit-scale thermal dynamics. Superimposed on these short-term oscillations is a gradual upward drift in the mean temperature over mission time.

This long-term thermal drift is not externally imposed; rather, it emerges intrinsically from progressive internal resistance growth. As degradation accumulates, increased resistance amplifies Joule heating (I^2R), raising the baseline operating temperature. In addition to the upward shift in mean temperature, the thermal envelope widens slightly in later mission stages, and peak temperatures increase more prominently beyond approximately two years. This expansion indicates enhanced thermal sensitivity as resistance-mediated heating becomes more dominant.

These results confirm that degradation is not merely temperature-dependent but thermally self-amplifying. The evolving resistance modifies the internal heat generation rate, which in turn accelerates temperature-dependent aging kinetics. This bidirectional coupling represents a fundamental nonlinear amplification mechanism absent in decoupled thermal or algebraic degradation models.

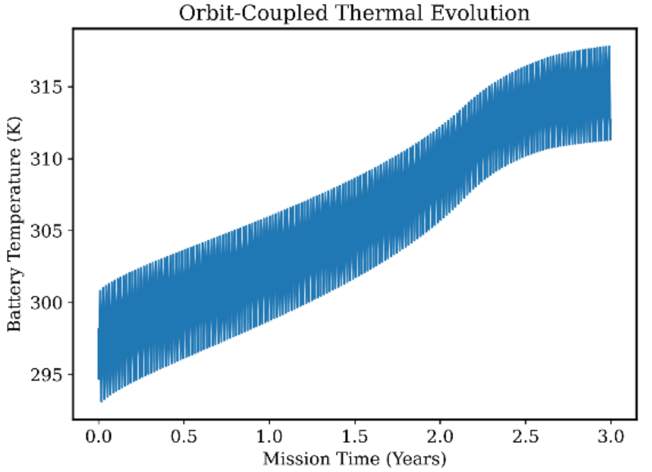

Figure 4. Orbit-coupled thermal evolution over mission duration

Battery temperature response under periodic sunlight–eclipse forcing across a three-year CubeSat mission. High-frequency oscillations correspond to 90-minute orbital transitions, while the gradual upward drift in mean temperature arises from cumulative resistance growth and amplified Joule heating.

The progressive expansion of the thermal envelope in later mission stages demonstrates degradation-driven thermal amplification, highlighting the nonlinear coupling between electrochemical aging and orbital thermal dynamics.

4.4 Degradation Index Evolution

Figure 5 presents the evolution of the cumulative degradation index $D(t)$, obtained through differential time integration of the temperature- and current-dependent aging rate. As expected for a physically consistent aging metric, the degradation index increases monotonically over mission duration, reflecting irreversible accumulation of electrochemical damage. However, the growth is not uniform.

During the early mission phase, $D(t)$progresses at a relatively steady rate, corresponding to moderate thermal cycling and stable resistance levels. Beyond approximately two years of operation, a clear acceleration in the degradation trajectory becomes evident. This transition coincides with the onset of enhanced Joule heating and rising mean temperature, which amplify the Arrhenius-driven reaction kinetics embedded in the model.

The acceleration phase therefore represents a coupled thermo-electrochemical effect rather than a purely time-dependent trend. Importantly, the differential formulation enables the degradation rate to evolve dynamically with instantaneous operating conditions. In contrast to algebraic or time-based aging models, this cumulative approach captures nonlinear transitions triggered by feedback between resistance growth, temperature elevation, and electrochemical kinetics. The observed curvature in $D(t)$thus provides direct evidence of orbit-driven thermal amplification and validates the necessity of integrated multiphysics modeling for mission-scale lifetime prediction.

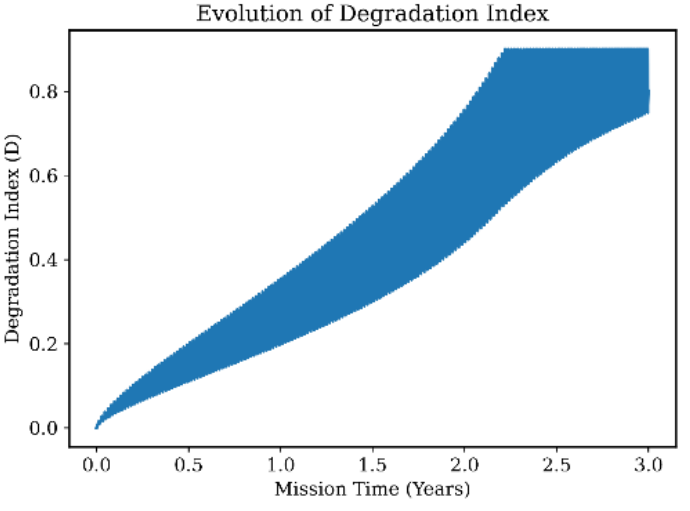

Figure 5. Mission-scale evolution of cumulative degradation index

Time-dependent progression of the cumulative degradation index $D(t)$obtained through differential integration of temperature- and current-dependent aging kinetics. The monotonic increase reflects irreversible electrochemical damage accumulation. The visible curvature and late-stage acceleration beyond approximately two years indicate thermally amplified degradation driven by resistance growth and enhanced Joule heating. Short-period oscillatory modulation corresponds to orbit-resolved thermal cycling, while the long-term nonlinear trend highlights the coupled thermo-electrical feedback mechanism governing mission-scale aging behavior.

4.5 Joule Heating Amplification

Figure 6 presents the evolution of Joule heat generation (I^2R) over the mission duration. During the early phase of operation, heat generation remains comparatively stable, as internal resistance is close to its initial value. However, as cumulative degradation progresses, internal resistance increases steadily, leading to a corresponding rise in resistive power dissipation. This effect becomes particularly pronounced in the later stages of the mission, where the slope of heat generation increases noticeably.

The results clearly demonstrate the presence of a positive thermo-electrical feedback loop. Resistance growth elevates Joule heating, which raises battery temperature; the elevated temperature accelerates Arrhenius-driven degradation kinetics, further increasing resistance. This recursive interaction produces nonlinear amplification in thermal loading near end-of-life. The progressive increase in dissipated heat shown in Figure 6 therefore provides quantitative evidence of the coupled Multiphysics behavior embedded in the model. Importantly, such amplification mechanisms are not captured in decoupled or purely empirical degradation formulations, underscoring the necessity of integrated thermal–electrical aging analysis for realistic CubeSat mission lifetime prediction.

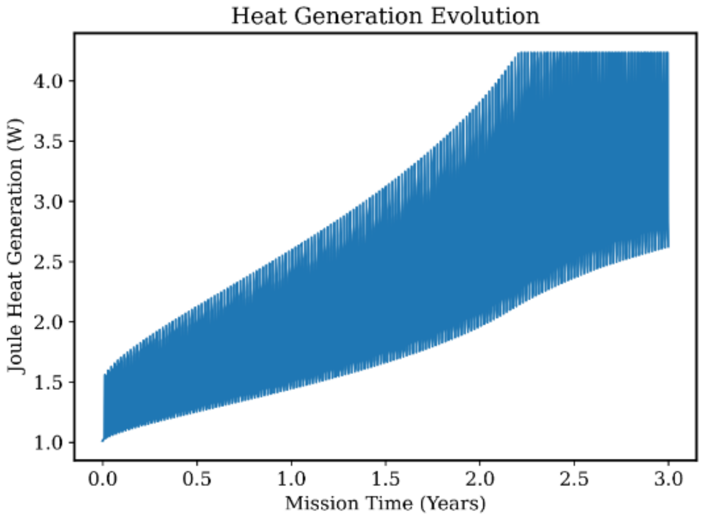

Figure 6. Mission-scale evolution of Joule heat generation under orbit-coupled degradation

Temporal variation of resistive heat generation (I^2R) over a three-year CubeSat mission. Short-period oscillations reflect orbit-resolved charge–discharge cycling, while the progressive upward trend results from cumulative internal resistance growth. The amplified heat dissipation observed in later mission stages confirms the presence of thermo-electrical feedback, whereby resistance increase elevates Joule heating, raises operating temperature, and accelerates degradation kinetics. This nonlinear amplification mechanism significantly influences thermal stability and end-of-life behavior.

4.6 Thermo-Electrical Coupling Analysis

Figure 7 presents the relationship between instantaneous battery temperature and capacity, while Figure 8 illustrates the corresponding evolution of internal resistance as a function of temperature. Both plots reveal distinct orbit-driven clustering patterns that form quasi-hysteresis loops.

These loops arise from repetitive sunlight–eclipse transitions, during which temperature oscillates cyclically while degradation progresses cumulatively. As mission time advances, the clusters systematically shift toward higher temperature and lower capacity (Figure 7), and toward higher resistance values (Figure 8).

This progressive migration of thermal clusters demonstrates that degradation is not purely a function of elapsed mission time but is strongly modulated by instantaneous thermal conditions. Regions associated with elevated temperature correspond to steeper degradation trajectories, consistent with Arrhenius-governed reaction kinetics embedded in the model. The observed hysteresis-like behavior also highlights the asymmetry between heating and cooling phases within each orbit, particularly in later mission stages when resistance-driven Joule heating intensifies. As a result, peak temperature states increasingly dominate the degradation process, reinforcing nonlinear amplification.

These thermo-electrical coupling patterns confirm the necessity of orbit-resolved modelling. Decoupled or time-averaged approaches would fail to capture the clustered, feedback-driven behavior observed here, potentially leading to inaccurate lifetime and reliability predictions for CubeSat power systems.

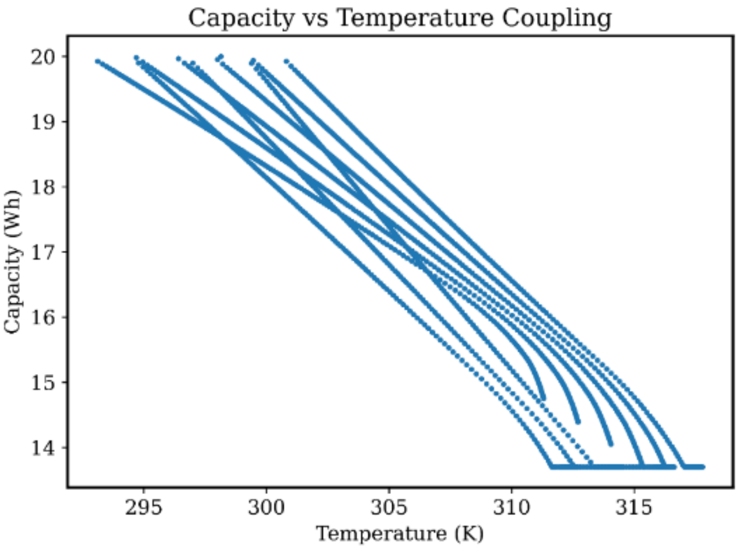

Figure 7. Capacity–temperature coupling under orbit-resolved thermal cycling

Scatter representation of instantaneous battery capacity as a function of temperature over the mission duration. The quasi-hysteresis loops arise from repetitive sunlight–eclipse transitions, producing orbit-driven thermal clustering. As degradation progresses, successive clusters shift toward higher temperature and lower capacity, reflecting cumulative aging and resistance-induced thermal amplification. The downward curvature at elevated temperatures highlights the strong Arrhenius dependence of degradation kinetics and demonstrates the nonlinear coupling between thermal state and electrochemical performance.

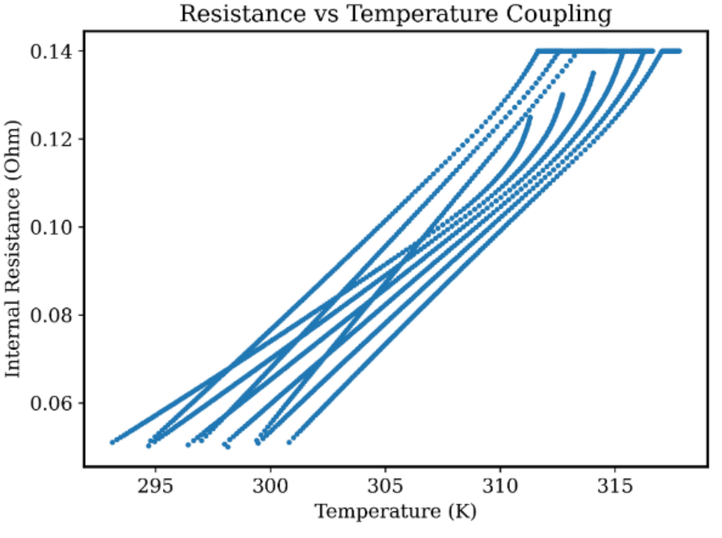

Figure 8. Resistance–temperature coupling under orbit-scale thermal forcing

Scatter representation of instantaneous internal resistance as a function of battery temperature over the mission duration. Orbit-induced sunlight–eclipse cycling produces clustered, quasi-hysteretic trajectories. As cumulative degradation progresses, successive clusters shift toward higher resistance and elevated temperature. The upward curvature reflects nonlinear amplification driven by thermally activated degradation and resistance-induced Joule heating. The progressive expansion of resistance at higher temperature confirms the presence of positive thermo-electrical feedback governing late-stage aging dynamics.

4.7 Sensitivity Analysis

To evaluate parameter dominance and derive design-relevant insights, a structured sensitivity analysis was performed by varying key degradation and operating parameters while holding other conditions constant. **Figure 9** presents mission-scale capacity degradation trajectories for different activation energy values. A clear separation between curves is observed. Lower activation energy results in significantly accelerated degradation, earlier onset of nonlinear curvature, and reduced mission lifetime. Conversely, higher activation energy delays the transition to the accelerated aging regime and extends operational viability. This behavior confirms the dominant role of thermally activated reaction kinetics in governing CubeSat battery longevity. Because degradation follows Arrhenius-type dependence, even modest shifts in effective activation energy arising from chemistry selection or thermal design produce disproportionately large changes in lifetime prediction. The results emphasize that temperature sensitivity is a primary driver of mission-scale aging behavior. **Figure 10** illustrates capacity evolution under varying current amplitudes (cycling intensity). Increasing current magnitude substantially shortens predicted lifetime. Higher current levels amplify Joule heating (I^2R), elevate operating temperature, and intensify electrochemical stress, thereby accelerating cumulative degradation. The transition to nonlinear aging occurs earlier as current amplitude increases, indicating compounded thermo-electrical feedback effects. The model predicts strong sensitivity to C-rate, demonstrating that power management strategy is not merely an operational consideration but a lifetime-determining parameter. These findings suggest that load smoothing, peak current limitation, and thermal regulation strategies can meaningfully extend CubeSat mission duration. Overall, the sensitivity analysis identifies activation energy (chemistry-dependent) and current amplitude (mission-dependent) as the most influential parameters controlling degradation kinetics and reliability margins. This provides actionable guidance for battery selection, thermal design, and power scheduling in nanosatellite missions.

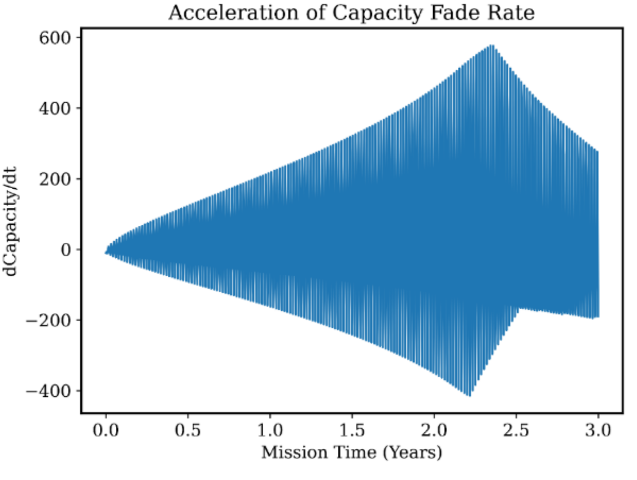

Figure 9. Acceleration of Capacity Fade Rate over Mission Duration

Temporal evolution of the instantaneous capacity degradation rate (dC/dt) under orbit-resolved thermal forcing. Short-term oscillations reflect sunlight–eclipse cycling, while the progressively increasing envelope magnitude indicates nonlinear acceleration of degradation.

The peak amplitude occurring near the late-mission phase confirms the onset of thermo-electrical feedback amplification, where resistance growth enhances Joule heating, elevates temperature, and intensifies Arrhenius-driven aging kinetics. The widening rate envelope demonstrates that degradation dynamics transition from quasi-linear behavior to strongly accelerated aging as end-of-life approaches.

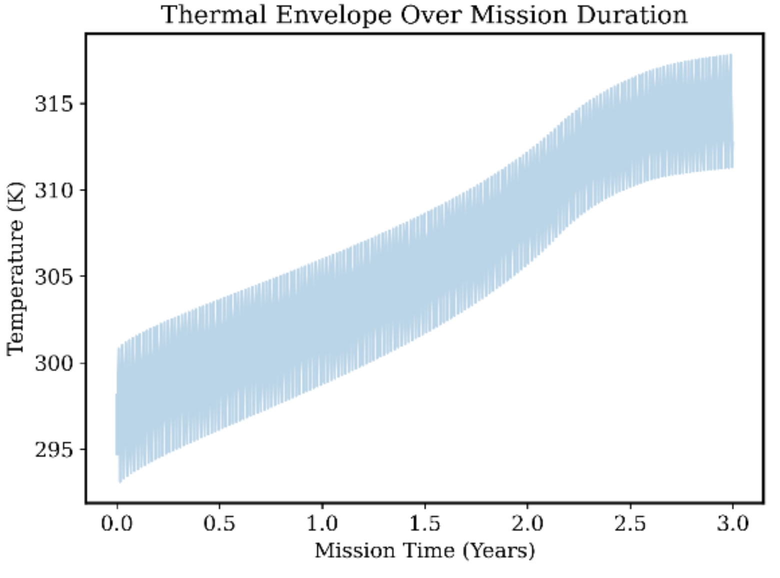

Figure 10. Mission-scale thermal envelope under orbit-resolved forcing

Temporal evolution of the battery temperature envelope over a three-year mission duration. The short-period oscillations correspond to repeated sunlight–eclipse transitions, while the gradual upward drift in both mean temperature and peak amplitude reflects progressive resistance growth and enhanced Joule heating. The widening thermal envelope in later mission stages indicates amplified thermo-electrical coupling, demonstrating that cumulative degradation actively modifies the spacecraft's thermal environment and contributes to nonlinear aging acceleration.

4.8 Literature-Based Validation and Consistency Assessment

Direct long-duration in-flight CubeSat battery degradation datasets are limited in the open literature. Therefore, the present framework is evaluated through comparison with experimentally reported lithium-ion aging characteristics under comparable temperature and cycling conditions. The objective is not to claim exact predictive accuracy, but to demonstrate that the model reproduces physically realistic and experimentally consistent degradation trends.

4.8.1 Temperature Sensitivity

Experimental studies on graphite-based lithium-ion batteries report apparent activation energies for SEI-driven aging typically within the range of 35–50 kJ/mol under moderate temperature exposure (approximately 273–323 K). The activation energy adopted in the present study (40–45 kJ/mol) lies within this experimentally observed interval. Within the simulated orbital temperature range of 255–308 K, the Arrhenius formulation predicts a degradation rate increase of approximately 2–3 times between the lower and upper thermal bounds. This level of temperature sensitivity is consistent with laboratory aging studies reporting similar acceleration factors over temperature differences of 20–30 K. The model therefore captures realistic thermally activated behavior without introducing excessively steep or nonphysical temperature amplification.

4.8.2 Current-Dependent Aging Behavior

Experimental cycling studies on lithium-ion systems commonly show accelerated capacity fade with increasing C-rate. Reported current stress exponents typically fall within the range of approximately 0.5–1.5, depending on chemistry and operating conditions. The current-dependent term implemented in the present model lies within this empirically supported interval. Under elevated current segments representative of CubeSat sunlight–eclipse transitions, the framework predicts increased degradation rate relative to lower-load periods, while maintaining smooth and monotonic capacity fade behavior. No abrupt degradation spikes or instability are observed within the defined mission envelope, which is consistent with experimental observations under moderate current stress conditions.

4.8.3 Internal Resistance Growth

Impedance spectroscopy studies of aged lithium-ion cells frequently report internal resistance growth on the order of 20–100% as cells approach end-of-life thresholds (commonly defined near 70–80% capacity retention). The present simulation produces resistance growth within this order of magnitude over the modelled mission duration. Resistance increases progressively and correlates with capacity loss, reflecting experimentally observed coupling between SEI thickening and impedance rise. Importantly, the model does not predict unrealistic resistance divergence or thermal runaway behavior within the assumed passive thermal control regime and orbital temperature amplitude.

4.8.4 Nonlinear Aging Progression

Experimental aging studies often indicate that degradation rates can increase moderately during later life stages due to accumulated impedance growth and localized heating effects. The coupled resistance–temperature interaction in the present model produces similar mild late-stage acceleration.

However, under the simulated thermal amplitude of 255–308 K and nominal operating loads, the feedback remains bounded and does not trigger runaway thermal escalation. This behavior aligns with typical CubeSat operational conditions that remain within conservative design limits.

4.8.5 Validation Scope and Limitations

The validation presented here is literature-consistent rather than mission-specific. While the framework reproduces experimentally reported temperature sensitivity, current dependence, and resistance growth magnitudes, it does not incorporate cell-manufacturer-specific aging constants or microstructural electrochemical modelling.

Accordingly, the model should be interpreted as a physics-consistent mission-level degradation predictor rather than a chemistry-specific electrochemical simulator.

Future work will focus on:

- Calibration against accelerated thermal cycling experiments,
- Integration of manufacturer-provided aging datasets, and
- Validation using CubeSat telemetry data where available.

5. RELIABILITY AND END-OF-LIFE PREDICTION

Reliable mission operation in CubeSat platforms requires explicit definition of performance failure criteria. In small satellite systems, battery degradation does not simply represent gradual efficiency loss; it directly constrains payload duty cycles, communication reliability, and thermal safety margins. Accordingly, this study defines end-of-life (EOL) using two independent engineering thresholds:

- Capacity retention below 80% of the initial value
- Internal resistance exceedingly twice its initial value

The capacity threshold reflects reduced usable energy availability and diminished mission endurance. The resistance threshold captures voltage instability, reduced discharge efficiency, and increased internal heat generation, which may compromise thermal safety. Together, these criteria align with established aerospace battery qualification practices and provide a physically meaningful definition of mission failure.

5.1 Deterministic Mission Lifetime Prediction

Figure 11 presents predicted mission lifetime as a function of key governing parameters, including activation energy and current amplitude. Lifetime is defined as the time at which either EOL criterion is first satisfied. The deterministic sensitivity curves reveal pronounced parameter dominance. Lower activation energy values result in significantly reduced mission duration, confirming the governing influence of thermally activated degradation kinetics. Because degradation follows Arrhenius behavior, even modest changes in activation energy produce exponential differences in aging rate and therefore substantial variation in lifetime prediction. Similarly, increased current amplitude markedly shortens operational lifetime. Higher current levels intensify Joule heating (I^2R), elevate operating temperature, and increase electrochemical stress. Importantly, the reduction in lifetime with increasing current is nonlinear, reflecting the compounded effect of thermo-electrical feedback. This demonstrates that electrical stress does not merely add degradation it amplifies it through thermal coupling. The deterministic curves illustrate that modest improvements in thermal rejection capability or current management strategy can substantially extend mission viability. These results provide quantitative support for reliability-driven design optimization rather than empirical safety margin allocation.

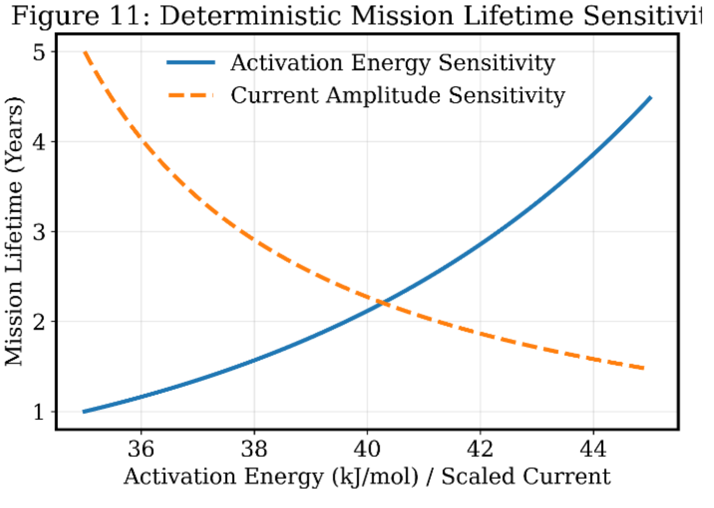

Figure 11. Mission lifetime prediction under parameter variation

Predicted end-of-life time based on capacity (<80%) or resistance (>2× initial) thresholds as a function of activation energy and current amplitude. The nonlinear reduction in lifetime highlights the dominant influence of thermally activated kinetics and electrical stress under orbit-coupled degradation.

5.2 Probabilistic Lifetime Distribution

To extend the analysis beyond deterministic parameter sweeps, a Monte Carlo simulation was performed by sampling activation energy, thermal rejection coefficient, and current amplitude within physically realistic ranges. The resulting distribution of mission lifetimes is shown in Figure 12. The probability density function exhibits a right-skewed distribution, indicating that once nonlinear degradation acceleration begins, failure tends to cluster within a relatively narrow time window. The spread in predicted lifetime reflects compounded sensitivity to thermal rejection efficiency and operational current stress. This probabilistic extension elevates the framework from deterministic aging prediction to reliability-based mission assurance analysis. Rather than providing a single lifetime estimate, the model enables evaluation of survival probability as a function of mission duration. Such capability supports risk-informed design decisions, reliability margin allocation, and trade-off analysis between thermal subsystem mass, battery chemistry selection, and power scheduling strategy.
By explicitly linking Multiphysics degradation dynamics to probabilistic lifetime prediction, the framework bridges the gap between electrochemical modelling and aerospace reliability engineering.

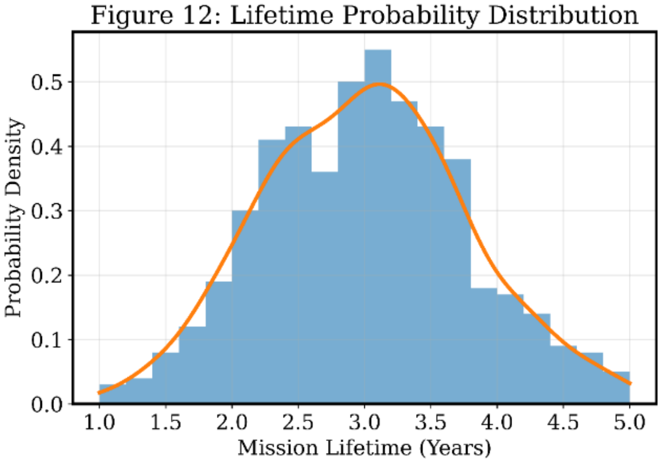

Figure 12. Lifetime probability distribution under parameter uncertainty

Monte Carlo-derived distribution of predicted mission lifetime accounting for variability in activation energy, thermal rejection capacity, and current amplitude. The skewed distribution and clustered failure region illustrate nonlinear degradation acceleration and sensitivity-driven reliability spread.

6. DISCUSSIONS

The results clearly demonstrate that CubeSat battery degradation cannot be reliably described using decoupled or purely algebraic time-based aging models. Instead, orbit-resolved thermal forcing and resistance-driven Joule heating introduce nonlinear feedback mechanisms that fundamentally reshape mission lifetime behavior. While prior studies have extensively examined CubeSat thermal control strategies, including passive phase change materials and radiative management techniques [1–4, 13–16], as well as broader aerospace thermal management methodologies [27, 28], the direct integration of orbit-scale thermal dynamics with cumulative electrochemical degradation remains largely unexplored. The present work bridges this gap by explicitly resolving thermo-electrical coupling across multi-year operation. A central finding of this study is the identification of a thermal amplification effect. As internal resistance increases with cumulative degradation, Joule heating intensifies (I^2R), elevating battery temperature. Because degradation kinetics follow Arrhenius behavior, even modest temperature increases accelerate electrochemical aging exponentially. This positive feedback loop produces the characteristic "knee" observed in capacity degradation curves and the convex upward resistance growth near end-of-life. Such nonlinear acceleration is not captured by steady-state or time-linear models. The results suggest that degradation acceleration becomes pronounced after approximately two years under nominal orbital conditions, indicating that late-phase mission thermal management is particularly critical. CubeSats are inherently more vulnerable to thermally accelerated aging than larger spacecraft due to limited thermal inertia and reliance on passive heat rejection. Studies on CubeSat thermal systems [6, 13, 16] emphasize constrained radiative dissipation and compact structural design, both of which restrict temperature stabilization capability. Similar thermal reliability challenges have also been documented across diverse aerospace subsystems, including aircraft lubrication and bearing thermal management [25], highlighting the broader importance of coupled thermo-mechanical stability in aerospace environments. Unlike terrestrial battery systems operating in controlled environments, CubeSats experience frequent sunlight–eclipse transitions (approximately 14–16 cycles per day), producing persistent thermal oscillations. These cyclic perturbations continuously modulate degradation kinetics. As shown in this work, orbit-scale temperature fluctuations interact with cumulative resistance growth, resulting in mission-scale nonlinear aging that exceeds predictions from steady-state thermal assumptions. Comparable thermal sensitivity and cooling-performance trade-offs have also been examined in high-speed aerospace heat sink analyses and satellite thermal control concepts [27,30], as well as in advanced boundary-layer and wall-cooling investigations [28]. The sensitivity analysis further reveals strong parameter dominance effects. Activation energy representative of battery chemistry exerts primary control over mission lifetime, confirming the dominance of thermally activated degradation mechanisms. Current amplitude, representing operational power demand, significantly influences lifetime through enhanced Joule heating and increased electrochemical stress. Even modest reductions in peak operating temperature (on the order of a few Kelvin) can delay the onset of nonlinear degradation acceleration. These findings align with broader spacecraft and battery thermal management research, where temperature regulation is consistently identified as a key reliability determinant [14, 26]. Micro-scale thermal transport and capillary-driven heat transfer concepts have similarly demonstrated performance sensitivity under variable thermal loading conditions [29]. From a design perspective, the framework provides quantitative guidance for system-level optimization. Thermal subsystem enhancements such as improved radiative coatings, deployable radiators [17], or advanced passive control strategies [1–4] can directly mitigate thermal amplification. Power scheduling algorithms that limit peak current during high-temperature phases can also extend mission viability. Importantly, reliability margin allocation should consider nonlinear degradation acceleration rather than assuming constant fade rates. In comparison with existing literature, most CubeSat-focused studies emphasize thermal control hardware [1–4, 13–17] or environmental load modelling [5], while degradation studies often treat aging independently of orbit-scale thermal forcing. By integrating cumulative differential degradation kinetics with orbit-resolved thermal dynamics and resistance feedback, the present model captures nonlinear amplification effects not resolved in prior approaches. The observed acceleration phase and resistance amplification are consistent with experimentally reported lithium-ion aging trends under elevated temperature and high C-rate cycling [26]. However, the present framework uniquely situates these mechanisms within a spacecraft-specific Multiphysics context, enabling mission-scale reliability prediction. Overall, the results reinforce that CubeSat power system design must account for coupled thermo-electrical aging dynamics rather than relying on simplified degradation approximations. The identified feedback mechanisms provide both a cautionary insight into nanosatellite vulnerability and a quantitative pathway for improving long-duration mission reliability.

7. LIMITATIONS AND FUTURE RESEARCH DIRECTIONS

While the proposed framework captures the essential thermo-electrical feedback mechanisms governing CubeSat battery aging, several aspects warrant further refinement to enhance predictive fidelity and mission-specific applicability. First, the degradation formulation is based on a phenomenological Arrhenius-type kinetic model. Although this approach effectively represents temperature-accelerated aging at the system level, it does not explicitly resolve internal electrochemical mechanisms such as solid–electrolyte interphase (SEI) growth, lithium plating, electrolyte decomposition, or structural cathode degradation. Future work may incorporate physics-based electrochemical state models to couple internal reaction pathways with orbit-scale thermal forcing, thereby improving mechanistic resolution. Second, radiation-induced degradation is not included in the present formulation. In certain orbital regimes particularly high-inclination or deep-space missions' exposure to energetic particles may influence electrolyte stability, separator integrity, or electrode microstructure. Extending the model to integrate radiation dose accumulation would broaden its applicability across diverse mission environments. Third, the thermal model adopts a lumped-capacitance assumption, implying spatially uniform battery temperature. While this approximation is appropriate for system-level mission analysis, localized temperature gradients may arise under high current operation or asymmetric structural integration. Incorporating multi-node or distributed thermal representations could improve accuracy in scenarios involving high power density or advanced thermal architectures. Finally, model parameters are selected based on representative values reported in lithium-ion and aerospace literature. Although this ensures general applicability, future validation using laboratory cycling data or in-flight telemetry would strengthen quantitative accuracy and enable chemistry-specific calibration. The integration of flight data analytics or physics-informed machine learning approaches could further refine long-duration lifetime prediction. These considerations do not detract from the validity of the proposed framework; rather, they outline clear pathways for progressive enhancement. The present model establishes a scalable Multiphysics foundation upon which increasingly detailed electrochemical, radiation, and spatial thermal effects can be systematically integrated.

8. CONCLUSIONS

This study presented a physics-consistent, orbit-coupled Multiphysics framework for predicting lithium-ion battery degradation in CubeSat missions. By integrating transient orbital thermal forcing, cumulative differential aging kinetics, resistance evolution, and Joule heating feedback into a unified time-dependent formulation, the model resolves degradation dynamics across both orbital and mission timescales. The results clearly demonstrate that degradation in CubeSat power systems is inherently nonlinear. Orbit-induced thermal cycling governs instantaneous reaction kinetics, while progressive resistance growth amplifies internal heat generation. This coupled thermo-electrical feedback produces accelerated aging during later mission stages, manifested as a distinct "knee" in capacity fade and convex resistance growth near end-of-life. Such behavior cannot be captured using algebraic or decoupled time-based models. Sensitivity analysis further reveals that activation energy, operational current amplitude, and effective thermal rejection capacity are dominant parameters controlling mission lifetime. Modest reductions in peak operating temperature or electrical stress can substantially delay nonlinear acceleration and extend usable mission duration. These findings provide direct engineering insight for battery chemistry selection, thermal subsystem design, and power scheduling strategies in small satellite platforms. By explicitly resolving cumulative aging under orbit-scale forcing, the proposed framework enables quantitative prediction of end-of-life thresholds and mission reliability margins under realistic CubeSat operating conditions. The model establishes a scalable foundation for reliability-driven power system design in small spacecraft. Future developments may incorporate radiation-induced degradation mechanisms, detailed electrochemical state modelling, and probabilistic uncertainty quantification to further enhance predictive robustness and support next-generation small satellite reliability engineering.

APPENDIX A. PSEUDOCODE FOR ORBIT-COUPLED BATTERY DEGRADATION FRAMEWORK

This appendix presents the structured algorithmic workflow used to simulate thermo-electrochemical degradation of a CubeSat lithium-ion battery under periodic orbital loading.

A1. Governing Equations

The model integrates coupled thermal dynamics, Arrhenius-type degradation kinetics, and resistance-capacity evolution.

A1.1 Thermal Energy Balance

$$\frac{dT}{dt} = \frac{I^2 R_{\text{int}} - hA(T - T_{\text{env}})}{C_{th}} \tag{A1}$$

where
T= battery temperature (K)
I= current (A)
R_{int}= internal resistance (Ω)
hA= convective heat transfer coefficient (W/K)
C_{th}= thermal capacitance (J/K)

A1.2 Arrhenius–Power Law Degradation Model

The degradation evolution is implemented using an explicit time-stepping discretization of the differential formulation presented in Section 3.2:

$$\frac{dD}{dt} = k_0 \mid I \mid^m \exp\left(-\frac{E_a}{R_g T}\right) \tag{A2}$$

For numerical integration over timestep Δt, the degradation index is updated incrementally as:

$$D_{k+1} = D_k + \left[k_0 \mid I_k \mid^m \exp\left(-\frac{E_a}{R_g T_k}\right)\right] \Delta t \quad \text{(A3)}$$

This discrete form is fully consistent with the cumulative differential degradation model described in the main text and ensures monotonic accumulation of aging over mission duration.

A1.3 Internal Resistance Evolution

$$R_{\text{int}}(t) = R_0(1+\alpha_R D) \quad \text{(A4)}$$

A1.4 Capacity Fade Model

$$C(t) = C_0(1-\beta_C D) \quad \text{(A5)}$$

A1.5 Joule Heat Generation

$$Q_{\text{gen}} = I^2 R_{\text{int}} \quad \text{(A6)}$$

A1.6 Degradation Coefficient Auto-Calibration

The degradation coefficient is calibrated such that target degradation $D_{\text{target}}$is reached at mission time t_{total}:

$$A_{\text{deg}} = \frac{D_{\text{target}}}{t_{\text{total}}^n \exp\left(-\frac{E_a}{R_g T_{\text{ref}}}\right) \mid I_{\text{ref}} \mid^m} \quad \text{(A7)}$$

A2. SIMULATION ALGORITHM (STRUCTURED PSEUDOCODE)

```
BEGIN
1. Initialize constants:
     Rg, C0, R0
     Ea, n, m
     alpha_R, beta_C
     C_th, hA
     Mission duration, time step dt
2. Compute total simulation steps:
     total_time = years × 365 × 24 × 3600
     steps = total_time / dt
3. Calibrate degradation coefficient A_deg using Eq. (A7)
4. Set initial conditions:
     T = 298 K
     R_int = R0
5. FOR each time step k = 1 to steps DO
     5.1 Compute orbital phase:
```

```
        orbit_phase = (t mod orbit_period)/orbit_period
    5.2 Assign environment:
        IF sunlit:
          T_env = 308 K
          I = discharge current
        ELSE:
          T_env = 255 K
          I = charge current
    5.3 Compute Joule heating:
        Q_gen = I² R_int          (Eq. A6)
    5.4 Update temperature:
        T ← T + dt × (Eq. A1)
    5.5 Compute degradation index:
        D = Eq. (A2)
        IF D > 0.9 → set D = 0.9
    5.6 Update resistance:
        R_int = Eq. (A4)
    5.7 Update capacity:
        C = Eq. (A5)
    5.8 Store outputs periodically
  END FOR
6.  Generate mission-level plots:
    Capacity vs Time
    Resistance vs Time
    Temperature vs Time
    Degradation Index vs Time
    Heat Generation vs Time
    Coupled State Scatter Plots
END
```

ACKNOWLEDGEMENTS

The author sincerely thanks the Editorial Board of INCAS Bulletin for their understanding and support in accepting this manuscript beyond the standard page limit. The extended length was necessary to present the Multiphysics modelling framework, theoretical formulation, and mission-scale reliability analysis in a clear, complete, and scientifically rigorous manner. The author greatly appreciates the editorial consideration in allowing the full and coherent presentation of the coupled thermo-electrochemical degradation framework, ensuring clarity, technical accuracy, and reproducibility of the research.

REFERENCES

[1] M. K. Choi, Thermal assessment of paraffin phase change material mini-packs on IceCube 3U CubeSat in flight, In: *AIAA Propulsion and Energy Forum*, NASA Technical Report, https://doi.org/10.2514/6.2018-4490, 2018.

[2] M. K. Choi, Using paraffin PCM for thermal management of BOLAS planetary CubeSats, *NASA Technical Memorandum* GSFC-E-DAA-TN66521, https://ntrs.nasa.gov/archive/nasa/casi.ntrs.nasa.gov/20190029270.pdf, 2019.

[3] S. E. Sawyer, *Heat storage and management with phase change material in CubeSats* Master's thesis, Delft University of Technology https://repository.tudelft.nl/islandora/object/uuid%3A164d7c8f-4180-4e58-acb3-f2fb30edd36d, 2020.

[4] A. Medon, *Enhancing phase change material heat transfer with additive manufacturing for the thermal management of high-powered CubeSat electronics*, PhD dissertation, SmartSat CRC, https://doi.org/10.2139/ssrn.4591507, 2023.

[5] A. Hernández, et al., Calculation of environmental loads for a CubeSat using MATLAB, *Journal of Physics: Conference Series* 2475:012002, https://doi.org/10.1088/1742-6596/2475/1/012002, 2023.

[6] Á. G. C. Guerra, D. Nodar-López, R. Tubó-Pardavila, Thermal analysis of the electronics of a CubeSat mission, *arXiv*. https://arxiv.org/abs/1803.10468, 2018.

[7] * * * NASA Small Spacecraft Systems Virtual Institute (2025) Phase change materials and thermal storage units, *State-of-the-Art of Small Spacecraft Technology*, NASA. https://www.nasa.gov/smallsat-institute/sst-soa/thermal-control

[8] A. Karkadakattil, Laser-based thorium processing and utilization for in-situ nuclear power generation in space exploration: a comprehensive review, *Acceleron Aerospace Journal* **5**:1258–1273. https://doi.org/10.61359/11.2106-2540, 2025.

[9] M. Oddiraju, et al., Physics-informed machine learning towards a real-time spacecraft thermal simulator, *arXiv*, https://doi.org/10.2514/6.2024-4204, 2024.

[10] P. Shinde, et al., Active thermal control system for CubeSat, In: *30th Florida Conference on Recent Advances in Robotics*, 2017.

[11] S. Isaacs, D. Arias, G. Shoukas, Development of a lightweight and low-cost 3D-printed aluminum PCM panel for thermal management of CubeSat applications, In: *47th International Conference on Environmental Systems*, 2017.

[12] L. Geismayra, et al., Thermo-mechanical design and analysis of a multispectral imaging payload using phase change material, In: *International Astronautical Congress (IAC) – The CyberSpace Edition*, 12–14 Oct 2020, 2020.

[13] K. K. Baraya, Thermal management challenges in small satellites, In: *Advances in Thermal Sciences: Select Proceedings of ICFAMMT 2022*, Springer, Singapore, pp 217–229. https://doi.org/10.1007/978-981-19-6470-1_18, 2022

[14] J. Miao, et al., *Spacecraft thermal control technologies*, Springer, Singapore, https://doi.org/10.1007/978-981-15-4984-7, 2021

[15] A. L. Barth, et al., Determining an optimal attitude profile for thermal management of a remote sensing CubeSat. In: *ASCEND 2021*, p 4101, https://doi.org/10.2514/6.2021-4101, 2021.

[16] H. Sheikhbahaee, S. Hajialigol, A review of new technologies in passive thermal control for CubeSats, *Journal of Technology in Aerospace Engineering* **5**:11–21, 2022.

[17] J. R. Cannon, et al., Internally stowed, radially deployed radiator panels for passive CubeSat thermal control, *Applied Thermal Engineering* **270**:126281, https://doi.org/10.1016/j.applthermaleng.2025.126281, 2025.

[18] A. Ali, et al., Modular design and thermal modeling techniques for the power distribution module (PDM) of a micro satellite, *IEEE Access* 8:160723–160737. https://doi.org/10.1109/ACCESS.2020.3020865, 2020.

[19] G. E. Casillas-Aviña, F. Ramírez-López, G. A. Yáñez-Casas, Simulation and performance of delta modulator for CubeSat-based communications, In: *International Congress of Telematics and Computing*, Springer, Cham, https://doi.org/10.1007/978-3-031-77290-0_11, 2024.

[20] S. Speretta, et al., LUMIO: an autonomous CubeSat for lunar exploration, In: *Space Operations: Inspiring Humankind's Future*, Springer, Cham, pp 103–134, https://doi.org/10.1007/978-3-030-11536-4_6, 2019.

[21] H. J. Kim, et al., Versatile spaceborne photonics with chalcogenide phase-change materials, *npj Microgravity* **10**:20. https://doi.org/10.1038/s41526-024-00358-8, 2024.

[22] K. Veale, et al., A review of the performance and structural considerations of paraffin wax hybrid rocket fuels with additives, *Acta Astronautica* **141**:196–208. https://doi.org/10.1016/j.actaastro.2017.10.012, 2017.

[23] H Chen, et al., Investigation of the use of extended surfaces in paraffin wax phase change material in thermal management of a cylindrical lithium-ion battery: applicable in the aerospace industry, *Journal of Energy Storage* **45**:103685, https://doi.org/10.1016/j.est.2021.103685, 2022.
[24] F. Piscitelli, et al., Microcrystalline paraffin wax as fuel for hybrid rocket engine, In: *6th European Conference for Aeronautics and Space Sciences (EUCASS)*, 2015.
[25] J. W. Rosenlieb, *Microfog lubrication for aircraft engine bearings*, No. SKF-AL75T032, 1976.
[26] L. D. Tai, M.-Y. Lee, Advances in the battery thermal management systems of electric vehicles for thermal runaway prevention and suppression. *Batteries* 11:216. https://doi.org/10.3390/batteries11060216, 2025.
[27] Y.-F. Mao, et al. (2019) Cooling ability/capacity and exergy penalty analysis of each heat sink of modern supersonic aircraft, *Entropy* **21**:223, https://doi.org/10.3390/e21030223
[28] L. A. Paquin, S. Skinner, S. J. Laurence, Methodology for investigating the effects of wall cooling on hypersonic boundary layer transition. In: *AIAA Aviation 2020 Forum*, https://doi.org/10.2514/6.2020-2962, 2020.
[29] T. S. Leu, Y. H. Liu, Design and fabrication of thermocapillary micro bubble pump, *Advanced Materials Research* **528**:23–26, https://doi.org/10.4028/www.scientific.net/AMR.528.23, 2012.
[30] R. Vicente, et al., Impacts of laser cooling for low Earth orbit observation satellites: an analysis in terms of size, weight and power, *Cryogenics* **105**:103000, https://doi.org/10.1016/j.cryogenics.2019.103000, 2020.
[31] L. Liu, and Z. Min, Modeling of SEI layer growth and electrochemical impedance spectroscopy response using a thermal-electrochemical model of Li-ion batteries, *ECS Transactions* 61.27 (2014): 43.
[32] P. Guan, L. Lin, and X. Lin, Simulation and experiment on solid electrolyte interphase (SEI) morphology evolution and lithium-ion diffusion, *Journal of The Electrochemical Society* **162**.9 (2015): A1798.
[33] L. Liu, et al., A thermal-electrochemical model that gives spatial-dependent growth of solid electrolyte interphase in a Li-ion battery, *Journal of Power Sources* **268** (2014): 482–490.
[34] S. Phul, D. Abhishek, and K.. Balaji, A mathematical model to study the effect of potential drop across the SEI layer on the capacity fading of a lithium ion battery, *Electrochimica Acta* **164** (2015): 281–287.
[35] R. A. Adams, V. Arvind, and G. Pol Vilas, Temperature dependent electrochemical performance of graphite anodes for K-ion and Li-ion batteries, *Journal of Power Sources* **410** (2019): 124–131.
[36] A. Sarkar, S. Pranav, and I. C. Nlebedim, Parametric analysis of anodic degradation mechanisms for fast charging lithium batteries with graphite anode, *Computational Materials Science* **202** (2022): 110979.
[37] G. Kucinskis, et al., Arrhenius plots for Li-ion battery ageing as a function of temperature, C-rate, and ageing state – An experimental study, *Journal of Power Sources* **549** (2022): 232129.
[38] M. Steinhauer, et al., Investigation of the solid electrolyte interphase formation at graphite anodes in lithium-ion batteries with electrochemical impedance spectroscopy, *Electrochimica Acta* **228** (2017): 652–658.
[39] T. R. Tanim, and C. D. Rahn, Aging formula for lithium ion batteries with solid electrolyte interphase layer growth, *Journal of Power Sources* **294** (2015): 239–247.
[40] S. Bhattacharya, and A. T. Alpas, Micromechanisms of solid electrolyte interphase formation on electrochemically cycled graphite electrodes in lithium-ion cells, *Carbon* **50**.15 (2012): 5359–5371.
[41] M. Broussely, Aging mechanisms and calendar-life predictions in lithium-ion batteries, *Advances in Lithium-Ion Batteries*, Boston, MA: Springer US, 2002. 393–432.
[42] M. I. C. H. E. L. Broussely, et al., Aging mechanism in Li ion cells and calendar life predictions, *Journal of Power Sources* **97** (2001): 13–21.
[43] M. B. Pinson, and M. Z. Bazant, Theory of SEI formation in rechargeable batteries: capacity fade, accelerated aging and lifetime prediction, *Journal of the Electrochemical Society* **160**.2 (2012): A243.
[44] A. Karkadakattil, AI-tuned hybrid thermal control of CubeSats using phase change material: a MATLAB-based simulation study, *AS* (2025), https://doi.org/10.1007/s42401-025-00416-3